Crosslinked actin networks show liquid crystal elastomer behaviour, including soft-mode elasticity

PAUL DALHAIMER[1,2], DENNIS E. DISCHER[2,3,4]* AND TOM C. LUBENSKY[3,4]*

[1]Molecular, Cellular, and Developmental Biology, Yale University, New Haven, Connecticut 06520-8103, USA
[2]Chemical and Biomolecular Engineering, University of Pennsylvania, Philadelphia, Pennsylvania 19104-6391, USA
[3]Physics and Astronomy Graduate Group, University of Pennsylvania, Philadelphia, Pennsylvania 19104-6396, USA
[4]Laboratory for Research on the Structure of Matter, University of Pennsylvania, Philadelphia, Pennsylvania 19104-6202, USA
*e-mail: discher@seas.upenn.edu; tom@dept.physics.upenn.edu

Published online: 18 March 2007; doi:10.1038/nphys567

Actin filament networks with protein crosslinks of distinct length and flexibility resemble liquid crystal elastomers. We simulate actin filament systems with flexible crosslinkers of varying length and connectivity to understand general phase behaviour and elasticity. Simulated networks with very short filaments and long crosslinkers resemble the cytoskeleton of the red blood cell and remain isotropic in compression and shear, seeming well-suited to blood flow. In contrast, networks with longer filaments as found in many cell types show three regimes of nematic phase behaviour dependent on crosslinker length: (1) 'loose' networks are isotropic at zero stress but align under compression or shear; (2) 'semi-loose' networks are nematic at low stress but become isotropic under dilation and (3) 'tight' networks possess a locked-in nematic order as represented by the cytoskeleton of the outer hair cell in the ear, for which anisotropic compliance directs sound propagation. Furthermore, for a subset of loose networks with 'periodic' connections among filaments, extremely soft stress–strain behaviour is found, as predicted for liquid crystal elastomers.

Cytoskeletal organization and elasticity are greatly influenced by molecular stiffness and sterics as well as externally imposed and internally generated stresses[1,2]—or so it might be hypothesized. These thermally dynamic networks are generally composed of stiff filaments of actin and flexible crosslinkers (Fig. 1a) that include filamin[3], spectrin[4] and many other proteins that are shorter or longer. In particular, cytoskeletons of the red blood cell (RBC)[5–7] and the outer hair cell (OHC)[8,9] in the ear (Fig. 1a, insets) are both composed of actin filaments confined to two dimensions at the plasma membrane and crosslinked by a brush of flexible spectrin (or perhaps filamin-like) chains (Fig. 1b). Here we use coarse-grained Monte Carlo simulations to map out the physically possible phase behaviour and elastic properties for a range of such networks.

Recent theoretical efforts describe density-dependent network phases of crosslinked rods[10] as well as distinct elasticity regimes of random networks of rigid rods in two dimensions[11,12]. Recent experiments have identified not only isotropic, nematic and raft phases[13] but also affine and non-affine elastic regimes of protein-crosslinked actin networks[14] and a dependence of network elasticity on the length of the crosslinker[15]. Two key issues that have not yet been studied, however, are the phase behaviour of such crosslinked network systems under shear and the elasticity effects and connectivity of the flexible crosslinks (here spectrin or filamin-like chains). Responses of networks to shear can be subtle: theories for elastomers with nematic order predict regimes of soft elasticity[16–20] that arise from the broken rotational symmetry of the nematic state, whereby the shear modulus in the plane containing the anisotropy axis vanishes such that, in certain geometries, small stress increments produce large strains as the nematic anisotropy axis rotates to relax stress. This behaviour is expected of a broader class of materials known as 'liquid crystal elastomers', which show typical liquid crystal phases, but have the elasticity of rubbery solids and thus will recover their shape after application of any type of stress (below yield). The requirements for this mode of elasticity in biological networks are unclear and must certainly start with an understanding of their phase behaviour.

Although cytoskeletons of the RBC, OHC and many other cells are similar to each other in composition, their connectivity and the relative contour lengths of their actin filaments (L_{actin}) and crosslinker chains (L_{X}) differ considerably[5,8]—as do their mechanical responses. In the RBC cytoskeleton, the elastic energy is dominated by the entropy of the spectrin chains. RBCs have a shear modulus $\mu \approx \rho_{\mathrm{X}} k_{\mathrm{B}} T$, with ρ_{X} being the number of spectrin chains per unit area[21–23], k_{B} the Boltzmann constant and T the temperature, thus the isotropic (I) short actin filaments seem to maintain the connectivity of the network but contribute negligibly to the elastic energy. Conversely, the OHC's micrometre-long, aligned actin filaments are likely to contribute substantially to the elastic energy and anisotropy[24] of its cytoskeleton. Between these two extreme examples of two-dimensional (2D) networks is a range of network structures, phases and elastic properties that we begin to map out here.

The phase behaviour of crosslinked actin networks is expected to be influenced strongly both by the filament aspect ratio, $L_{\mathrm{actin}}/D_{\mathrm{actin}}$, and by the length ratio of filament to crosslink, $L_{\mathrm{actin}}/L_{\mathrm{X}} \equiv \chi$. Nematic phases (N) are of course uniaxial with distinct elastic properties in the directions parallel and perpendicular to a suitable nematic order parameter. A first

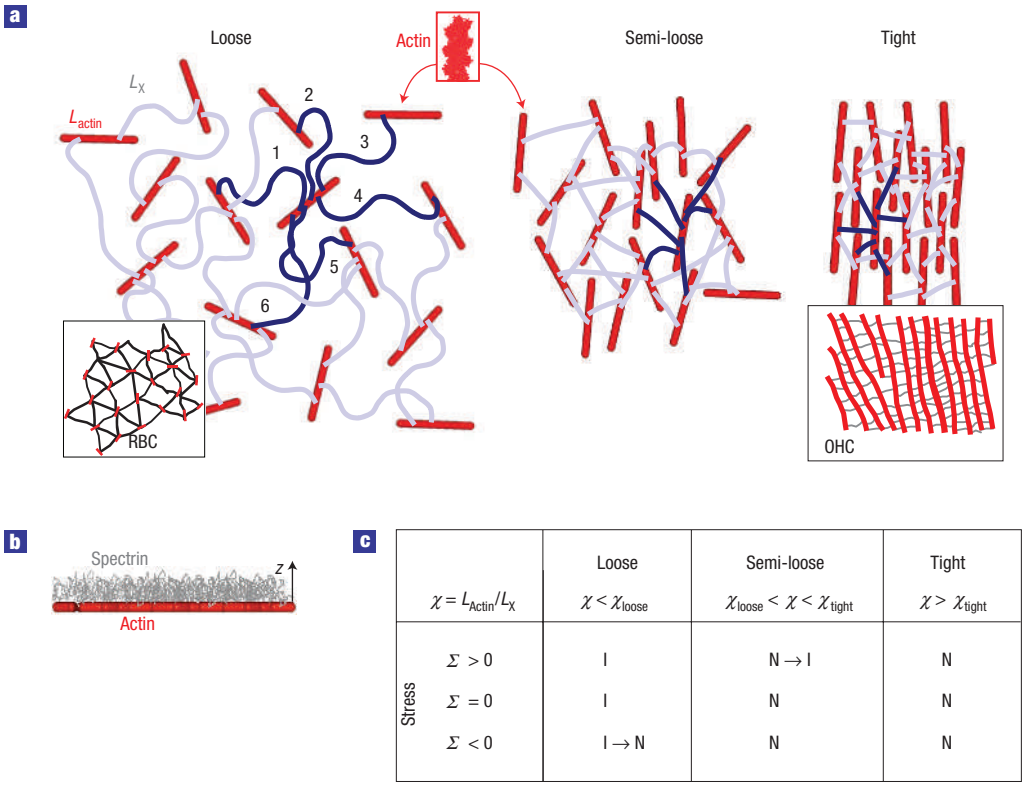

Figure 1 Prototypical membrane cytoskeletons with crosslinked actin filaments. a, Loose, semi-loose and tight networks represent networks with increasing L_{actin}/L_X ($\equiv \chi$). Loose networks with short filaments model the RBC cytoskeleton shown in the lower left inset[5] with red actin sketched in. Tight networks model the OHC cytoskeleton shown in the lower right inset[39]. **b**, Simulated systems consist of slightly bendable filaments[38] confined to a plane and crosslinked by six highly flexible chains extending as a brush away from the plane. **c**, Isotropic (I) and nematic (N) phases anticipated for the three types of network under isotropic stress (Σ).

requirement is that filament aspect ratio exceeds a critical length η: that is, $L_{actin}/D_{actin} > \eta$ is required for a nematic. If this condition is satisfied, then further consideration of the stresses required to generate nematic order suggests three possible regimes of network structure that we refer to here as 'loose', 'semi-loose' and 'tight' (Fig. 1a,c). Loose networks are defined by $\chi < \chi_{loose}$, and produce an isotropic phase unless compressed ($\Sigma < 0$) or sheared into a nematic phase. Semi-loose networks possess $\chi_{loose} < \chi < \chi_{tight}$, and are nematic unless expanded ($\Sigma > 0$), although shear may or may not induce disorder. Semi-loose networks are almost certainly found in subsets of cytoskeletons in highly dynamic cells as visualized by electron microscopy[25,26]. Tight networks are always nematic with $\chi > \chi_{tight}$ and describe the uniaxial network of the OHC as well as other bundle-filled networks. The nematic order parameter in two dimensions is given by $S_{actin} = \langle \cos 2\theta \rangle$ as calculated from the angle θ that an actin filament makes with the direction of average order[27]. A key aim here is to map out network phase behaviour together with the less predictable range of elastic properties possible—including soft elastic modes based on filament rotation. As theoretical approaches for understanding actin dynamics emerge[28,29], the results here can provide a new framework for categorizing and elucidating key collective features.

THE MODEL

We simulate, as simply as possible, the statistical mechanics of thermally fluctuating[30], crosslinked actin networks under stress as relevant to cell deformability, cell crawling and other cytoskeletal functions. Actin filaments (see Fig. 1a and Supplementary Information, Fig. S1a) are stiffened by a bond-angle potential and studied as lengths of $L_{actin} \sim 3$–$80\ D_{actin}$. Distinct from past simulations of fluids of rods and of course central to a cytoskeleton, the actin filaments are crosslinked with flexible bead-on-string chains (~5 nm diameter) that idealize network connectivity. Six crosslinking spectrin chains are permanently attached at distinct random sites along each actin filament (Fig. 1b, blue crosslinkers; see Supplementary Information), and so we refer to the connectivity as quasi-C_{6v} as it lacks any true rotational symmetry in crosslink attachment. This randomness in attachment contrasts with a distinct 'periodic' attachment simulated in the final part of this paper, which imposes a crystalline type of crosslinking with rotational symmetry such that knowledge of how one filament is crosslinked to adjacent filaments is sufficient to generate an entire network. The networks studied have either self-avoiding spectrin chains (Net-1) or else chains that can cross through each other (Net-2 and Net-3), but no significant differences were seen in the behaviours of networks with these different spectrin models. Future work could incorporate non-equilibrium dissociation of the crosslinkers or disruption of the filaments, but here we focus on equilibrium behaviour. The coarse-grained Monte Carlo simulations are conducted in constant-$n\Sigma T$ ensembles with periodic boundary conditions, where n denotes the total number of beads in the network[22,31]. The simulation results demonstrate the broad effects of actin filament and crosslinker length on the structure and properties of various cell cytoskeletons.

RESULTS

COMPRESSION AND EXPANSION OF LOOSE NETWORKS ($L_{actin}/L_X < \chi_{loose}$) VERSUS FLUIDS

For loose networks where isotropic phases are accessible at $\Sigma = 0$ (Fig. 1a), filament aspect ratio L_{actin}/D_{actin} is the primary determinant of network phase behaviour under compressive stresses ($\Sigma < 0$). The phase diagram of our networks (Fig. 2a, filled symbols) under compression maps reasonably well onto that of 2D fluids of spherocylinders[27], where ν_{actin} is the area of one actin filament (Fig. 2a, open symbols and lines). On compression of a thermally equilibrated isotropic state (I), networks with $L_{actin}/D_{actin} \leq 6$ (per RBC) undergo a discontinuous transition to a glass (G) with locally ordered domains (that is, I → G: Fig. 2d → b). The latter phase is identified by a hysteresis in ρ_{actin} on expansion and recompression from a crystalline configuration[27] (see Supplementary Information, Fig. S2).

The same isotropic compression of loose networks with $L_{actin}/D_{actin} \geq 11$ results in alignment of the filaments into stable nematic phases (I → N), which we identify by $S_{actin} \geq 0.5$, as defined elsewhere[27]. Four separate networks show such phase behaviour with increasing values of L_{actin}/D_{actin} (Fig. 2a, filled squares). Configurations of a network with $L_{actin}/D_{actin} \approx 11$ show the difference in filament alignment at high (Fig. 2c) versus low (Fig. 2e) density.

2D fluids of rods[27] show continuous transitions (N ↔ I) for long rods and discontinuous transitions from dense crystalline states (C ↔ I) for short rods[32]. The networks here show surprisingly similar phase behaviour. On dilation from crystalline states, loose networks with $L_{actin}/D_{actin} \leq 6.5$ show a dramatic drop in S_{actin} at C → I, indicative of a first-order transition (Fig. 2f, triangles) and have large, unstable fluctuations in S_{actin} at nematic densities. On the other hand, and as an extreme case, very thin filaments with $L_{actin}/D_{actin} \approx 80$ show a smooth decrease in S_{actin} at expected transition densities, consistent with the continuous transition for long-rod fluids[27] (Fig. 2f, circles). We do not study the specific details of these transitions beyond their observed (dis)continuities here and refer the reader to ref. 32 for a rigorous treatment of 2D phase transitions, including the seemingly relevant Kosterlitz–Thouless vortex-unbinding mechanism. Although the system sizes here are small—even in two dimensions—and cannot capture phase coexistence among other interesting macroscopic phenomena, the results thus far illustrate the remarkable similarity in compression of filament networks and hard-rod fluids, but of course equilibrium tension and shear should prove more divergent.

PHASE DIAGRAM FOR LOOSE NETWORKS UNDER COMPRESSION PLUS SHEAR

Unlike fluid systems, crosslinked networks equilibrate under shear. Here, we imposed shear on networks by elongating the periodic box in the 1-direction by a factor λ_1 (that is, $l_1 \rightarrow \lambda_1 l_1$) while compressing in the 2-direction ($l_2 \rightarrow \lambda_2 l_2$) to keep the overall area (and ρ_{actin}) of the box constant ($\lambda_1\lambda_2 \approx 1$ and $\Delta\rho_{actin} \approx 0$). A shear strain is expressed as $1/2(\lambda_1/\lambda_2 - 1) = 1/2(\lambda_1^2 - 1)$. Configurations of networks with $L_{actin}/D_{actin} \approx 11$ at different shear values illustrate the change in actin filament order (see Supplementary Information, Fig. S3a→c). Shear acts as an aligning field for nematic order and does not cause the jamming problems occasionally observed in compression of networks with ($6.5 < L_{actin}/D_{actin} < 11$). Indeed, networks with $L_{actin}/D_{actin} \geq 6.5$ are readily sheared from isotropic to highly ordered states. Easy alignment of filaments in shear perhaps in part explains why dynamic cytoskeletons exploit branching factors such as the Arp2/3 complex that transfer shear to neighbouring filaments[33].

The importance of crosslinker length in short-filament (RBC) networks is made clear in shear ($\Delta\rho_{actin} \approx 0$) with anisotropic stresses Σ_{para} and Σ_{perp} applied parallel and perpendicular to the direction of actin alignment. Note that this mode of deformation is referred to as pure shear and differs from the more conventional simple shear ($x \rightarrow x + \gamma y$ and $y \rightarrow y$) by a kinematic rotation and by the constant density constraint. With networks having the

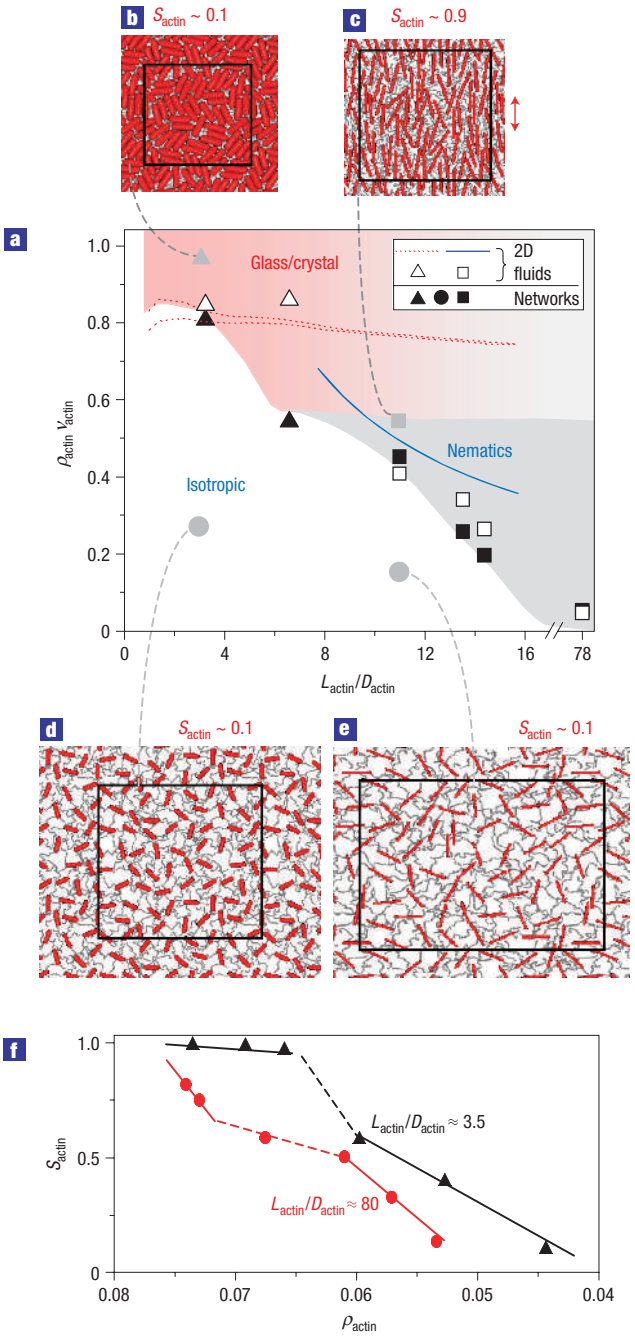

Figure 2 Density-dependent phase behaviour for loose networks and uncrosslinked fluids as a function of L_{actin}/D_{actin} with $L_{actin}/L_X < \chi_{loose}$. **a**, Lines indicate I–G/C or I–N transitions of 2D hard-rod fluids[27]. Simulations here yield similar transitions for both fluid systems (open triangles and open squares) and networks (filled triangles, filled circles and filled squares). Nematic order (N) is seen for $(L_{actin}/D_{actin}) > \eta$ with $\eta \cong 7$. **b–e**, Configurations show compression from an isotropic configuration to either a glass for short-filament networks (**b** ← **d**), or a nematic for long-filament networks (**c** ← **e**). **f**, Distinct density-driven transitions (dashed lines) in S_{actin} are seen for short- and long-filament networks.

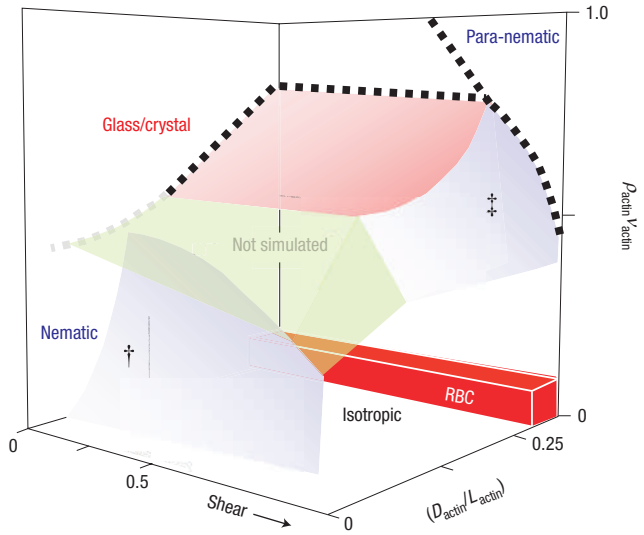

Figure 3 Phase diagram with shear for loose networks ($L_{actin}/L_X < \chi_{loose}$). Shearing of networks with $L_{actin}/D_{actin} > 8$ produces the tilted blue surface (†), above which filaments are nematically ordered ($S_{actin} > 0.5$) and below which they are isotropic ($S_{actin} < 0.5$). Short-filament networks ($L_{actin}/D_{actin} \leq 6.5$) near the glass transition can also be aligned under large shear and are referred to here as para-nematics (‡). The long spectrin chains of the RBC dominate actin interactions even at high compression and high shear (red box).

longest crosslinkers simulated and $L_{actin}/D_{actin} \approx 3.5$ (ref. 31), shear from the zero-stress state shows negligible ordering of filaments (see Supplementary Information, Fig. S3d→e)—even at shears considerably higher than those experienced by an RBC squeezing through a capillary[34]. This result confirms fluorescence polarization experiments on RBCs, where no filament order is observed when shear is imposed with a micropipette[31]. In theory, shear and nematic order of 'any' rods are coupled, and shear should produce rod alignment[20], but for short rods the coupling is so weak that alignment is negligible except at extreme shears that are not physiologically relevant[28,35].

We constructed a phase diagram for networks under both shear and isotropic stresses (Fig. 3). Although the phase diagram of loose networks of rods under zero shear is almost identical to that of 2D fluids of rods, equilibrium shear alignment of the networks from isotropic densities drives an I→N transition (Fig. 3, light blue surfaces). Networks with $L_{actin}/D_{actin} > 6.5$ yield an I→N transition surface in shear, which shows less pronounced curvature with increasing L_{actin}/D_{actin}. For $(L_{actin}/D_{actin}) \approx 11$ and $(L_{actin}/L_X) < \chi_{loose}$, the actin density couples to the shear stress response (see Supplementary Information, Fig. S3). Indeed, as described below, at sufficiently high ρ_{actin} and with particular types of crosslinking the filaments interact sufficiently with each other to cause the networks to be soft[16–19] and to rotate their director as a dominant elastic mode.

NEMATIC BEHAVIOUR OF LOOSE, SEMI-LOOSE AND TIGHT NETWORKS

Networks with L_{actin}/D_{actin} large enough to produce nematic phases are either loose, semi-loose or tight as defined by the stress required (if possible to achieve) for the N→I transitions. These regime boundaries are demarcated by two red vertical lines in Fig. 4a at the length ratios of χ_{loose} and χ_{tight}. Values for S_{actin} were calculated for networks with $L_{actin}/D_{actin} \approx 9$ or 10 (Fig. 4a, squares or triangles, respectively)and L_X ranging from $13\sigma_X$ to $40\sigma_X$ at several values of stress near $\Sigma = 0$. In the extreme case of infinite crosslinker length (that is, a 2D fluid of actin filaments), the stress needed to induce nematic order is similar to that found previously[27]: $\Sigma = -0.1k_BT/\sigma_X^2$. In loose networks, the filaments are disordered at $\Sigma = 0$, and compression is required to produce the nematic phase (Fig. 4a, open symbols). Nematic order at $\Sigma = 0$ is also achieved when filaments are interconnected by crosslinkers where $L_{actin}/L_X > \chi_{loose}$ (Fig. 4a, filled squares). Given spectrin chain lengths of 200 nm (ref. 4), the results here imply nematic order at $\Sigma = 0$ with actin filaments of length 120 nm or more. This is several times the unit filament length found in RBC[5] (35 nm) but much shorter than actin filament lengths in OHC. In addition, the spectrin-family crosslinker, α-actinin, has a length of only about 30 nm and thus requires only 18-nm-long actin filaments to order. This may explain the strong tendency of filamentous actin to order near membrane focal adhesions where short α-actinin crosslinkers predominate[36].

ELASTICITY AND ANISOTROPY OF LOOSE, SEMI-LOOSE AND TIGHT NETWORKS IN SHEAR

Nematic networks should show anisotropic elasticity. Possible models for this elasticity are uniaxial solids, which strongly resist shear of any kind, and thermotropic nematic elastomers[16], which show varying degrees of soft[17–19] elasticity. Soft nematic elastomers are idealized phases that develop nematic order from an isotropic phase and thereby spontaneously break a continuous symmetry. Their shear modulus vanishes for simple shears of $x \rightarrow x + \gamma y$ and $y \rightarrow y$, where y is taken along the nematic anisotropy or parallel direction (that is, in the direction of S_{actin}). In addition, finite strains of $1/2(\lambda_{perp}^2 - 1)$ in the perpendicular direction to the nematic director can in theory be produced with zero stress. The latter phenomenon arises because the filaments can rotate to relieve stress. Thus the compliance J_{perp} for stress along the perpendicular direction is in theory infinite whereas J_{para}—for stresses in the parallel direction—is finite. Synthetic nematic elastomers studied to date form polydomain[16] rather than monodomain samples and thus show a complicated elastic response. Certain classes of nematic elastomers show soft elasticity: the nematic elastomers are uniaxial solids at small strain with $J_{perp} > J_{para}$, and at larger strains their perpendicular stress–strain curves show a plateau in which the slope of Σ_{perp} versus λ_{perp} is small or zero, which is the result of filament rotation. The structural requirements for such behaviour in the present types of network are revealed below.

Responses of networks with various values of L_{actin}/L_X were studied under directional stress. Loose networks were compressed to the same density as tight networks, at which point $S_{actin} \sim 1$. The strain measure here uses $\lambda_{perp_0} \approx 1$, and $\lambda_{para} = 1/\lambda_{perp}$. The tight, locked network ($L_{actin}/L_X = 1.37$) is stiffened at low strain by stretched crosslinkers ($\mu_0 \gg \rho_X k_B T$), and its stress quickly diverges at the limit of chain extensibility (Fig. 4b, filled black diamonds; Fig. 4c →d). This network remains ordered with $S_{actin} > 0.5$, characteristic of a uniaxial solid (Fig. 4b, filled blue diamonds). The loose network ($L_{actin}/L_X = 0.46$) is more supple, with a stress–strain curve that is compatible with a uniaxial elastomer having a small J_{para} and large J_{perp} (Fig. 4b, open black squares). Its filaments rotate strongly, albeit not in the same direction, in response to stress, to produce a configuration where $S_{actin} < 0.5$ (Fig. 4b, open blue squares). The rotation of the actin filaments in this network is different from that required to achieve a completely soft elastic response, as distinguished below. Thus, in these non-periodically crosslinked networks, increased compliance, or softness, at relatively large strains is more dependent on the length of the crosslinker than the alignment of actin filaments.

We measured both the parallel and the perpendicular compliances—at small strains—of the four networks represented by the squares in Fig. 4a and the network represented by the

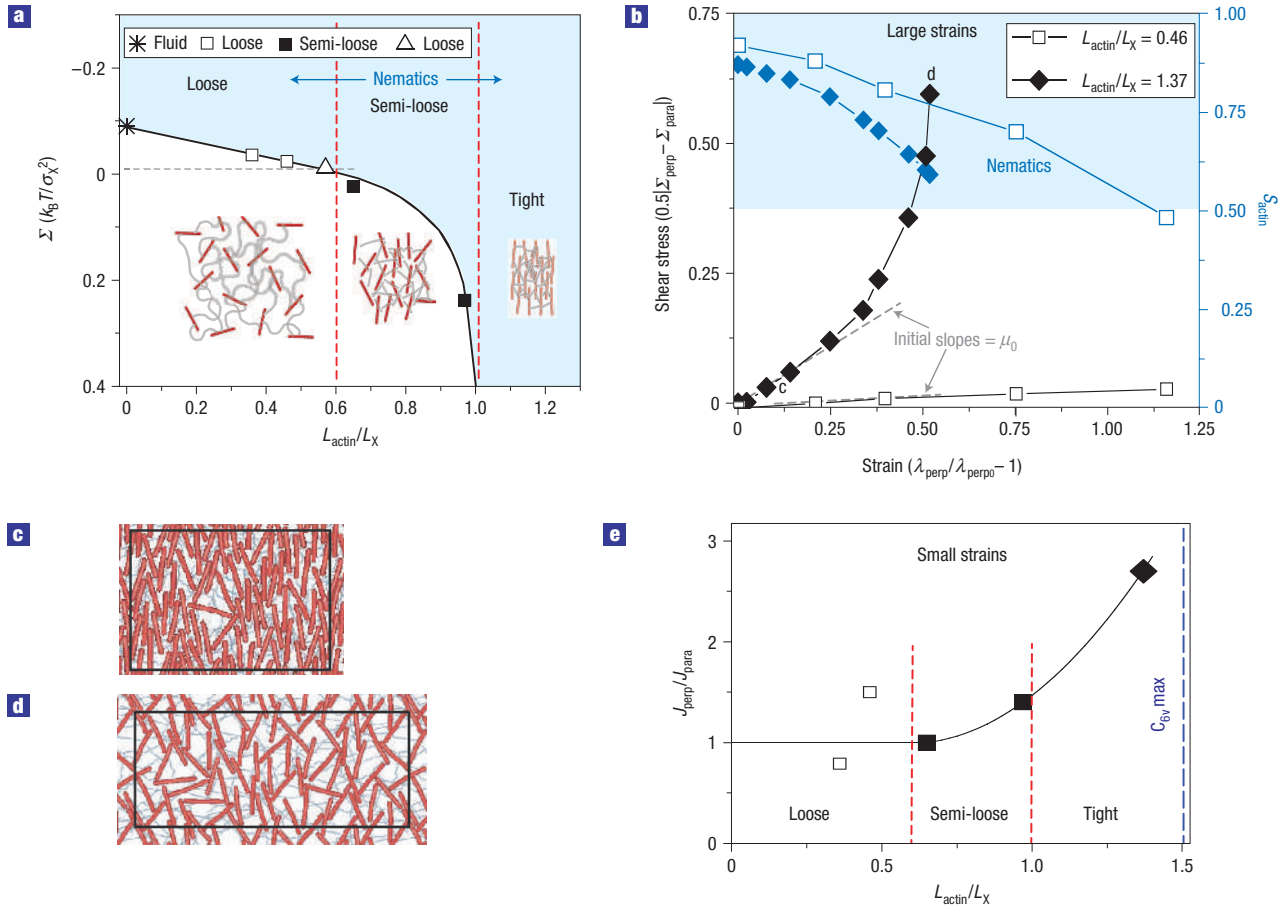

Figure 4 Effects of L_X on networks with $L_{actin}/D_{actin} > \eta$. **a**, With crosslinkers of various lengths, three regimes emerge, as demarcated by dashed red lines at $L_{actin}/L_X \approx 0.6$ ($\equiv \chi_{loose}$) and 1.0 ($\equiv \chi_{tight}$). Loose (open squares and open triangle) and semi-loose (filled squares) networks can become isotropic; tight networks cannot. The triangle represents networks with $L_{actin}/D_{actin} \approx 10$. The asterisk indicates a fluid of actin filaments: $L_X = \infty$. **b**, Shear stresses and S_{actin} of networks subjected to extension perpendicular to S_{actin} in either the loose (open squares) or tight regime (filled diamonds). **c**,**d**, Initial and final configurations, respectively, of the network with $L_{actin}/L_X = 1.37$. **e**, Tight networks show directional compliance (J).

filled diamonds in Fig. 4b. The goal was to explore possible anisotropy that emerges from the tight OHC type of cytoskeleton. As mentioned above, these five networks have $L_{actin}/D_{actin} \approx 9$ and are pre-compressed to the same area density but have different values for L_{actin}/L_X. The ratio J_{perp}/J_{para} increases with L_{actin}/L_X with a function that is well fitted by a shifted quadratic of form $y = 1 + a(x - x_0) + b(x - x_0)^2$ for $x \geq x_0$ ($x_0 = 0.65$, $a = 0.36$, $b = 2.8$); for $x \leq x_0$, $y = 1$ (Fig. 4e). This curve is incompatible with strictly soft behaviour, which predicts $J_{perp}/J_{para} \to \infty$, but it does show that the ratio J_{perp}/J_{para} increases as the system becomes tighter and nematic order increases. The value of $J_{perp}/J_{para} \sim 1$ in the semi-loose networks indicates that isotropic crosslinking surprisingly dominates the elastic response in spite of the nematic order, as seen for the larger strain simulations of loose and tight networks (Fig. 4b). Consistent with results for J_{perp}/J_{para}, box fluctuations for a nematic network at $\Sigma = 0$ with $L_{actin}/L_X \approx 1.37$ reveal a twofold greater value in amplitude of fluctuations in the direction perpendicular versus parallel to the aligned actin filaments (not shown). Hence, the value of L_{actin}/L_X plays an important role in the elasticity of these networks and possibly points to a reason for the relatively short spectrin crosslinkers in the OHC, since the hair cells are under low strains when transmitting sound, which is the regime in which the actin filaments seem to dominate the elasticity (Fig. 4e, diamond). Finally, experimental measurements indicate $J_{perp}/J_{para} \approx 6$ (ref. 24) for the OHC, and so assuming the connectivity here is representative the approximately threefold difference in perp/para elasticity for ~300 nm filaments here (Fig. 4e) is in good agreement with experiment, and simple extrapolation (to sixfold) would suggest an average filament length of ~500 nm in the OHC, which appears reasonable with images from experiment[8,9].

PERIODIC CONNECTIVITY OF CROSSLINKERS AND SOFT-MODE ELASTICITY

Left unstudied until this point is the possible role of the connectivity of the network crosslinkers to the actin filaments. Although each short actin filament in the RBC has six spectrin crosslinkers attached (ignoring defects), their connectivity to each filament is random and non-periodic. We therefore constructed three large networks (Net-2A, B and C), all in the loose regime, with 256 actin filaments and $L_{actin}/D_{actin} \approx 9$. As is the case with all networks studied here up until this point, Net-2A has non-periodic connectivity of spectrin to each actin filament. Net-2B lacks a bending energy for the actin filaments and is thus a crosslinked 'rubber'[22]. Important in contrast, Net-2C has periodic connections

of crosslinkers to the actin filaments that are identical in every 'filament unit cell' (see Supplementary Information, Fig. S1c). Since a soft response, if it exists, should occur at constant area, the density was constrained with $\lambda_{para}\lambda_{perp} \approx 1$. Thus, when we apply a stress Σ_{perp}, we adjust Σ_{para} to impose the constraint. Since Net-2A and Net-2C are isotropic at $\Sigma = 0$, all three networks were isotropically compressed to the same density, where Net-2A and Net-2C had $S_{actin} \sim 1$, and the elastic responses were assessed in shear. At subsequent low strains—up to about 25% extension—all networks showed the same crosslinker-density-dependent elasticity as predicted from simple theory: $\mu_0 \sim \rho_X k_B T$ (Fig. 5a). Net-2A and B both show the usual stiffening at moderate to high strain (Fig. 5a, open and filled squares; Fig. 5b →c).

Contrasting with the results above, Net-2C with periodic connectivity shows a very shallow slope from strains of 0.25–1.25 (Fig. 5a, triangles). This softening coincides with collective actin filament rotation with a stable value for S_{actin} (Fig. 5a, blue triangles; Fig. 5d →e) as theory predicts for soft nematic elastomers[16,18,20,37]. This collective rotation is clearly distinct from that observed in Fig. 4c →d for non-periodic crosslinking of actin filaments. In addition, although the filaments in Net-2A rotate, they do so in a complex, almost prohibitive, manner with counter-acting torques that arise due to random connectivity (not so much sterics; see Supplementary Information, Table S1) and frustrate in driving $S_{actin} \to 0$ (Fig. 5a, filled blue squares; Fig. 5b →c).

These simulations provide strong evidence for the existence of soft elasticity in periodically (and presumably low-defect) crosslinked actin networks with nematic order. Thus, not only are the lengths of the filaments and the density of crosslinkers important to the structure and elastic responses of networks, but the detailed connectivity of the crosslinkers to the filaments is at least as important. Indeed, synthetic nematic elastomers composed of monodomains show softer elastic responses than those consisting of polydomains[16]. Moreover, an actin filament[38] has precise sites of association for actin binding proteins such as filamin, spectrin, actinin and many other crosslinking proteins, and so the tendency to create periodic networks is even more pronounced than with synthetic systems.

For further comparison to theory, the angle dependence of planar mesogens in shear ($r = \lambda_1/\lambda_2$) is described for an affine rotation[31] by $\varphi_{affine} = \cos^{-1}[(r^{-2}\sin^2\varphi_{r=1} + \cos^2\varphi_{r=1})^{-1/2}\cos\varphi_{r=1}]$, where φ is defined in ref. 31 by $\varphi = \pi/2 - \theta$. The actin filament angular distribution after stretching Net-2C from $r = 1$ to 6 is different from distributions of computed θ_{affine} (Fig. 5f, blue → purple versus blue → green). The network's filaments rotate to a greater extent (about twofold) and more collectively with less dispersion, consistent with a tendency for soft modes.

Crosslinked actin networks show shear- and density-dependent phases and anisotropies that are typical of liquid crystal elastomers, but perhaps the most intriguing response is the soft-mode elasticity of Fig. 5. Thus the key questions for future experiments on cytoskeletal structures and rheology concern not only phase and density under stress (Figs 2–4) but also perhaps connectivity, defects and 'periodicity' in crosslinking as well as collective rotations of filaments (Fig. 5). In particular, crosslinking that cooperates with filament rotation rather than frustrating it can produce extraordinarily soft responses (Fig. 5b,c versus 5d,e). Further theoretical work on dissociating crosslinkers that unbind or rebind under stress could be particularly interesting in either frustrating or perhaps cooperating with particular phases as well as novel elastic modes. Of course, timescales for interaction and force-dependent dissociation laws probably need to be known better to add this additional level of complexity to the already complicated responses observed here. Field theories of liquid crystal elastomers could prove insightful in capturing such effects[18–20].

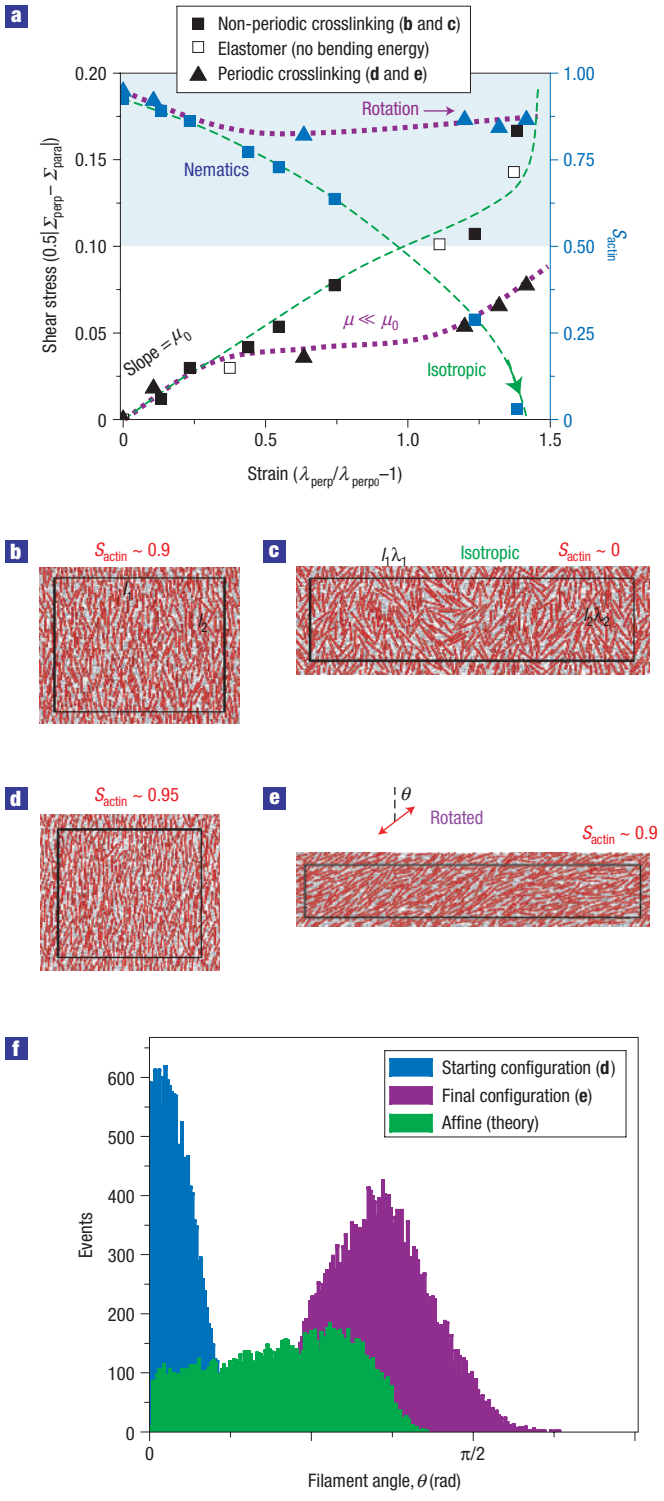

Figure 5 The nature of network crosslinking plays a key role in response to shear. a, Shear stress and S_{actin} (blue) of three different loose networks subjected to extension perpendicular to the direction of initial alignment ($L_{actin}/D_{actin} \approx 9$). Networks with random crosslinking (**b**,**c**) show no net rotation of their director and also show the same stress–strain response as a network lacking filaments (filled squares versus open squares). In contrast, networks with periodic crosslinking (**d**,**e**) show a soft plateau in stress (filled triangles). **f**, Affine predictions (green) underestimate the simulation's filament rotations (purple) after stretching from $r = 1$ (blue) → 6.

Received 13 September 2006; accepted 12 February 2007; published 18 March 2007.

References

1. Keller, M., Tharmann, R., Dichtl, M. A., Bausch, A. R. & Sackmann, E. Slow filament dynamics and viscoelasticity in entangled and active actin networks. *Phil. Trans. R. Soc. Lond. Ser. A* **361**, 699–711 (2003).
2. Uhde, J., Keller, M., Sackmann, E., Parmeggiani, A. & Frey, E. Internal motility in stiffening actin–myosin networks. *Phys. Rev. Lett.* **31**, 268101 (2004).
3. Wang, K., Ash, J. F. & Singer, S. J. Filamin, a new high-molecular-weight protein found in smooth-muscle and non-muscle cells. *Proc. Natl Acad. Sci. USA* **72**, 4483–4486 (1975).
4. Speicher, D. W. & Marchesi, V. T. Erythrocyte spectrin is comprised of many homologous triple helical segments. *Nature* **311**, 177–180 (1984).
5. Byers, T. J. & Branton, D. Visualization of the protein associations in the erythrocyte-membrane skeleton. *Proc. Natl Acad. Sci. USA* **82**, 6151–6157 (1985).
6. Debreuil, R., Byers, T. J., Branton, D., Goldstein, L. S. & Kiehart, D. P. Drosophila spectrin 2. conserved feaures of the alpha-subunit are revealed by analysis of cDNA clones and fusion proteins. *J. Cell Biol.* **105**, 2095–2102 (1987).
7. Welch, M. D., Holtzman, D. A. & Drubin, D. G. The yeast actin cytoskeleton. *Curr. Opin. Cell Biol.* **6**, 110–119 (1994).
8. Holley, M. C. & Ashmore, J. F. A cytoskeletal spring in cochlear outer hair-cells. *Nature* **335**, 635–637 (1988).
9. Wada, H. *et al.* Imaging of the cortical cytoskeleton of guinea pig outer hair cells using atomic force microscopy. *Hearing Res.* **187**, 51–62 (2004).
10. Borukhov, I., Bruinsma, R. F., Gelbart, W. M. & Liu, A. J. Structural polymorphism of the cytoskeleton: a model of linker-assisted filament aggregation. *Proc. Natl Acad. Sci. USA* **102**, 3673–3678 (2005).
11. Wilhelm, J. & Frey, E. Elasticity of stiff polymer networks. *Phys. Rev. Lett.* **91**, 108103 (2003).
12. Head, D. A., Levine, A. J. & MacKintosh, F. C. Distinct regimes of elastic response and deformation modes of cross-linked cytoskeletal and semiflexible polymer networks. *Phys. Rev. E* **68**, 061907 (2003).
13. Gardel, M. L. *et al.* Elastic behavior of cross-linked and bundled actin networks. *Science* **304**, 1301–1305 (2004).
14. Wong, G. C. *et al.* Lamellar phase of stacked two-dimensional rafts of actin filaments. *Phys. Rev. Lett.* **91**, 018103 (2003).
15. Wagner, B., Tharmann, R., Haase, I., Fischer, M. & Bausch, A. R. Cytoskeletal polymer networks: The molecule structure of cross-linkers determines macroscopic properties. *Proc. Natl Acad. Sci. USA* **103**, 13974–13978 (2006).
16. Warner, M. & Terentjev, E. M. *Liquid Crystal Elastomers* 1st edn (Oxford Univ. Press, Oxford, 2003).
17. Golubovic, L. & Lubensky, T. C. Nonlinear elasticity of amorphous solids. *Phys. Rev. Lett.* **63**, 1082–1085 (1989).
18. Warner, M., Blandon, P. & Terentjev, E. M. Soft elasticity—Deformation without resistance in liquid-crystal elastomers. *J. Phys. II (France)* **4**, 93–102 (1994).
19. Olmsted, P. D. Rotational invariance and Goldstone modes in nematic elastomers and gels. *J. Phys. II (France)* **4**, 2215–2230 (1994).
20. Lubensky, T. C., Mukhopadhyay, R., Radzihovsky, L. & Xing, X. Symmetries and elasticity of nematic gels. *Phys. Rev. E* **66**, 0112095 (2002).
21. Discher, D. E., Boal, D. H. & Boey, S. K. Phase transitions and anisotropic responses of planar triangular nets under large deformation. *Phys. Rev. E* **55**, 4762–4772 (1997).
22. Boey, S. K., Boal, D. H. & Discher, D. E. Simulations of the erythrocyte cytoskeleton at large deformation. I. Microscopic models. *Biophys. J.* **75**, 1573–1583 (1998).
23. Boal, D. H. Computer-simulation of a model network for the erythrocyte cytoskeleton. *Biophys. J.* **67**, 521–529 (1994).
24. Tolomeo, J. A., Steele, C. R. & Holley, M. C. Mechanical properties of the lateral cortex of mammalian auditory outer hair cells. *Biophys. J.* **71**, 421–429 (1996).
25. Pollard, T. D. & Borisy, G. G. Cellular motility driven by assembly and disassembly of actin filaments. *Cell* **112**, 453–465 (2003).
26. Otomo, T. *et al.* Structural basis of actin filament nucleation and processive capping by a formin homology 2 domain. *Nature* **433**, 488–494 (2005).
27. Bates, M. A. & Frenkel, D. Phase behavior of two-dimensional hard rod fluids. *J. Chem. Phys.* **112**, 10034–10041 (2000).
28. Carlsson, A. E. Structure of autocatalytically branched actin solutions. *Phys. Rev. Lett.* **92**, 238102 (2004).
29. Carlsson, A. E. The effect of branching on the critical concentration and average filament length of actin. *Biophys. J.* **89**, 130–140 (2005).
30. Lee, J. C.-M. & Discher, D. E. Deformation-enhanced fluctuations in the red cell skeleton with theoretical relations to elasticity, connectivity, and spectrin unfolding. *Biophys. J.* **81**, 3178–3192 (2001).
31. Picart, C., Dalhaimer, P. & Discher, D. E. Actin protofilament orientation in deformation of the erythrocyte membrane skeleton. *Biophys. J.* **79**, 2987–3000 (2000).
32. Kosterlitz, J. M. & Thouless, D. Ordering, metastability and phase-transitions in 2 dimensional systems. *J. Phys. C* **6**, 1181–1203 (1973).
33. Amann, K. J. & Pollard, T. D. Direct real-time observation of actin filament branching mediated by Arp2/3 complex using total internal reflection fluorescence microscopy. *Proc. Natl Acad. Sci. USA* **98**, 15009–15013 (2001).
34. Noguchi, H. & Gompper, G. Shape transitions of fluid vesicles and red blood cells in capillary flows. *Proc. Natl Acad. Sci. USA* **102**, 14159–14164 (2005).
35. Picart, C. & Discher, D. E. Actin protofilament orientation at the erythrocyte membrane. *Biophys. J.* **77**, 865–878 (1999).
36. Hu, K., Ji, L., Applegate, K. T., Danuser, G. & Waterman-Storer, C. M. Differential transmission of actin motion within focal adhesions. *Science* **315**, 111–115 (2007).
37. Disch, S., Schmidt, C. & Finkelmann, H. Nematic elastomers beyond the critical point. *Macromol. Rapid. Commun.* **15**, 303–310 (1994).
38. Holmes, K. C., Popp, D., Gebhard, W. & Kabsch, W. Atomic model of the actin filament. *Nature* **347**, 44–49 (1990).
39. Holley, M. C. & Ashmore, J. F. Spectrin, actin and the structure of the cortical lattice in mammalian cochlear outer hair-cells. *J. Cell Sci.* **96**, 283–291 (1990).

Acknowledgements

Support from Penn's NSF-MRSEC and from NIH and NSF grants is gratefully acknowledged.
Correspondence and requests for materials should be addressed to D.E.D. or T.C.L.
Supplementary Information accompanies this paper on www.nature.com/naturephysics.

Author contributions

P.D., D.E.D. and T.C.L. designed the research problem and wrote the manuscript; P.D. wrote and conducted the simulations.

Competing financial interests

The authors declare no competing financial interests.